JOURNAL OF THEORETICAL
AND APPLIED MECHANICS
4, 38, 2000

A FINITE ELEMENT MODEL FOR ABRASIVE WATERJET MACHINING

ASHRAF I. HASSAN
JAN KOSMOL

Department of Machine Technology, Silesian University of Technology, Gliwice
e-mail: jk@kbm.mt.polsl.gliwice.pl

This paper presents a first attempt to model abrasive waterjet (AWJM) machining process using the powerful tool of the finite element method (FEM) in order to explain the abrasive particle-workpiece interaction. The new model takes into account precise representation of the constitutive behaviour of the workpiece material under AWJ dynamic loading conditions which was ignored in previous AWJM models. In the present model, forces acting on the abrasive particle need not be initially determined, as in previous AWJM studies, as they are automatically calculated at each time step. The results show that the finite element method is a useful tool in predicting abrasive-material interaction and AWJ depth of cut.

Key words: waterjet machining, finite element method

1. Introduction

Abrasive waterjet machining (AWJM) has been successfully used in machining of a wide variety of engineering materials. The capabilities and applications of this new promising process are discussed in detail elsewhere (Hashish, 1984b; Hassan and Kosmol, 1997, Hoogstrate et al., 1997). Due to the large number of parameters involved in AWJM, a predictive model is crucial for optimization of the process performance. To understand and predict the AWJM performance, several models were developed. Most of these models were concentrated on prediction of the depth of cut and the surface quality, given the initial machining parameters. These models were based either on mathematical relationships describing the interaction between one abrasive

particle and the workpiece in the cutting and deformation wear zones (Zeng and Kim, 1996; Hashish, 1984a, 1988, 1989; Paul at al., 1998), or on experimental formulas based on the statistical design principles (Chen et al., 1998; Siores et al., 1996). The drawbacks of the early Hashish's model were: the abrasive particle velocity was assumed to be constant along the whole depth of the cut, the effects of the particle shape and size were ignored (Hashish, 1984a). In a subsequent study (Hashish, 1989), these effects were considered by expressing the sphericity and the roundness numbers of the abrasive particle. Moreover, the width of a cut was considered to be the same as the jet diameter. The accuracy of the predictive AWJM models, e.g. Hashish's model, was tested only on materials with similar general behaviour. In addition, all the published formulas require specific coefficients, which have to be determined experimentally. This means that the impact velocity, impact angle and grain size distribution are not accurately evaluated (Blickwedel et al., 1991). The common drawback of the previous models is that precise representation of the constitutive behavior of the workpiece material, under AWJ dynamic loading conditions, was ignored. The finite element method has been successfully applied in modeling of low-speed impact problems. For speeds less than 0.1 m/s, no significant waves will be produced, and hence the process can be regarded as occurring under quasi-static conditions. This impact is characterized by a completely elastic behavior, and the energy loss is a small portion of the total mechanical energy and can be neglected (Goldsmith, 1999). Up to date, there have been few attempts at analyzing the WJM using the powerful tool of the finite element method. A preliminary effort of modeling pure waterjets using a finite element model was carried out by Hassan and Kosmol (1998). Using this model, it was possible to predict the shape of the AWJ kerf, workpiece deformations and stresses.

The objective of this paper is to conduct a finite element analysis of the workpiece material under the action of AWJ. The new model takes into account a precise representation of the constitutive behaviour of the workpiece material under AWJ dynamic loading conditions which was ignored in previous AWJM models where the flow stress was represented by a constant value. Additionally, deformations and stresses occurring in the workpiece material in the vicinity of the cutting interface as a result of the erosion impact by AWJ could be obtained. In the previous AWJM studies, forces acting on the abrasive particle are assumed in order to determine the depth of cut. In the present model these forces need not be initially determined, as they are calculated at each time step. In the present model, the dynamic progress of the abrasive-workpiece interaction will be tracked at small time increments.

2. Finite element model

It is important that the finite element mesh should be fine enough to allow realistic deformation. Meshes that are too coarse can prohibit actual deformation and yield erroneous results. In the present study, the following assumptions are relevant:

- The hydrostatic loading plays a secondary role in the cutting process, i.e. the effect of the carrying fluid is only to accelerate the abrasive particle to high speeds (Hashish, 1984a).

- The abrasive particle velocity is recalculated at the beginning of each time step. This is contrary to the constant abrasive particle velocity assumed in previous studies (Hashish, 1984a).

- For the FE code to remain stable, the time step must subdivide the shortest natural period in the mesh. This means that the time step must be smaller than the time taken for a stress wave to cross the smallest element in the mesh. The time step is chosen as $0.01\,\mu$s.

- Loading resulting from the changes in motion is computed and applied internally.

- In this study, particle disintegration in the mixing chamber is neglected.

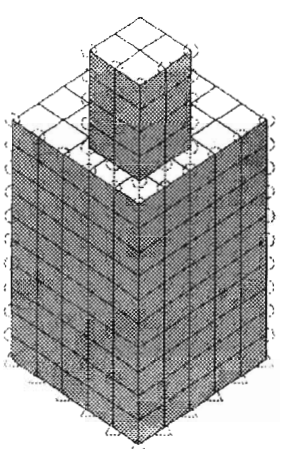

Fig. 1. Finite element model of AWJM

Figure 1 shows the finite element mesh adopted in the present study. The workpiece is modeled by a three-dimensional finite element model and is divided into 20 nodded, higher order nonlinear solid elements. A total number of 250 elements were used to model the workpiece with size of each element of 0.1mm × 0.1mm × 0.1mm. The number of nodal points is 1566. The overall workpiece dimensions are 0.5mm × 1mm × 0.5mm. The workpiece material data is shown in Table 1 below. In AWJM, the workpiece exhibits nonlinear material behavior and geometric nonlinearity under the applied impact loads, hence a nonlinear analysis is required. The constitutive model used for the workpiece is chosen as the von Mises elastoplastic isotropic hardening with linear strain hardening. This material model has more realistic response due to hardening and provides a simple means of accounting for the material response due to a stress reversal. Using this model, the workpiece erosion is shown simultaneously on the screen. The abrasive particle is modeled using 16 twenty nodded solid elements. Linear elastic model is chosen for the abrasive particle material. The dimensions of each element are 0.1mm × 0.1mm × 0.1mm. The AWJ cutting conditions are shown in Table 1. The boundary conditions include a fixed support of the workpiece from the bottom as it is fixed on the table of the AWJ machine. The abrasive particle is allowed to move freely downwards, perpendicularly to the workpiece surface.

Table 1

Workpiece material data		Abrasive material data		AWJM conditions	
Material	Carbon steel	Material	Garnet	Abrasive particle velocity [m/s]	400
Young's modulus	207 GPa	Young's modulus	248 GPa		
Poisson's ratio	0.3	Poisson's ratio	0.27	Abrasive particle size [μm]	400
Density	7850 kg/m^3	Density	4325 kg/m^3		
Yield stress	207 MPa			Mesh No.	60
Strain hardening modulus	34.5 GPa			Stand off distance [mm]	0.1
Specifications of 3D contact elements					
Contact area [mm^2]	Compressive contact distance	Number of elements	Type of nonlinear analysis	Material model	
0.01	0.01	9	Updated Lagrangian formulation	Bi-linear contact forcedistance law	

Preliminary investigations were carried out on several models and a compromise between the excessive CPU time and the accuracy of results was considered. 3D contact elements, the specifications of which are shown in Table 1, are added between the abrasive particle and the workpiece that allow for a complete interaction, including transfer of momentum between the abrasive particle and the workpiece. Contact elements are characterized by element

nonlinearity where the stiffness matrix of an element will change as a function of some specified variable. When the surfaces are in contact, the stiffness matrix of the contact element is positive, and the contact forces are transferred through the contact element. When the surfaces are not in contact, the stiffness of the contact element is zero and no forces are transferred.

The model was then analyzed on a Pentium II PC workstation and deformations and stresses in the workpiece material were obtained using the ALGOR Accupak/VE nonlinear dynamic stress analysis and event simulation, Version 12 WIN, which models the nonlinear behavior by increasing the load and updating the geometric stiffness matrix. In Event Simulation, the force is indeterminate and results from some type of action and motion. The deformation is calculated directly from the governing equations. In the AWJM, the advantage of this is that the user does not have to assume a static situation or to estimate values for AWJ impact forces. The analysis formulation used is the Updated Lagrangian Formulation, which is effective for modeling the elastic-plastic analysis involving large displacement, large rotation and large strain.

The constitutive relations are expressed in terms of the Jaumann stress rate and velocity strain tensors. At various critical loading points, extreme small time steps may be required in order to make an iterative process converge. At a large strain level, the generalized Hook's law (constant E, γ, etc.) no longer represents any real materials since the stress-strain relation is nonlinear. In large strain nonlinear analysis, the constitutive tensor is given in terms of certain material parameters which are functions of strains or stresses. Completely erroneous results may be generated if the material model is not consistent with the strain level of the structure. Large strain analysis is also used where geometric stiffness changes are expected. These conditions are typical for AWJM. The elastic-plastic model has the advantages of handling the geometric nonlinearity and instability and calculation of residual stresses, contrary to the rigid-plastic model which does not account for geometric nonlinearity and instability. The nonlinear iterative solution scheme used is the Combined Full and Modified Newton-Raphson Iteration Algorithm. It is between the full Newton-Raphson method, which has the advantages of being usually more effective for problems with strong nonlinearity such as AWJM, and since it converges quadratically with the number of iterations, and the Modified Newton-Raphson method, which is suitable for moderate nonlinearity and is not effective for sudden loading condition changes such as those encountered in AWJM. This solution method allows to achieve convergent solutions for problems involving motion. This solution method damps out the

common convergence problems such as high frequencies, because they are just noise within the solution.

3. Results and discussion

As AWJ hits the workpiece surface, an erosion front develops. The cutting front is moving through the workpiece material. The development of workpiece deformation as a result of AWJ impact is shown in Fig.2.

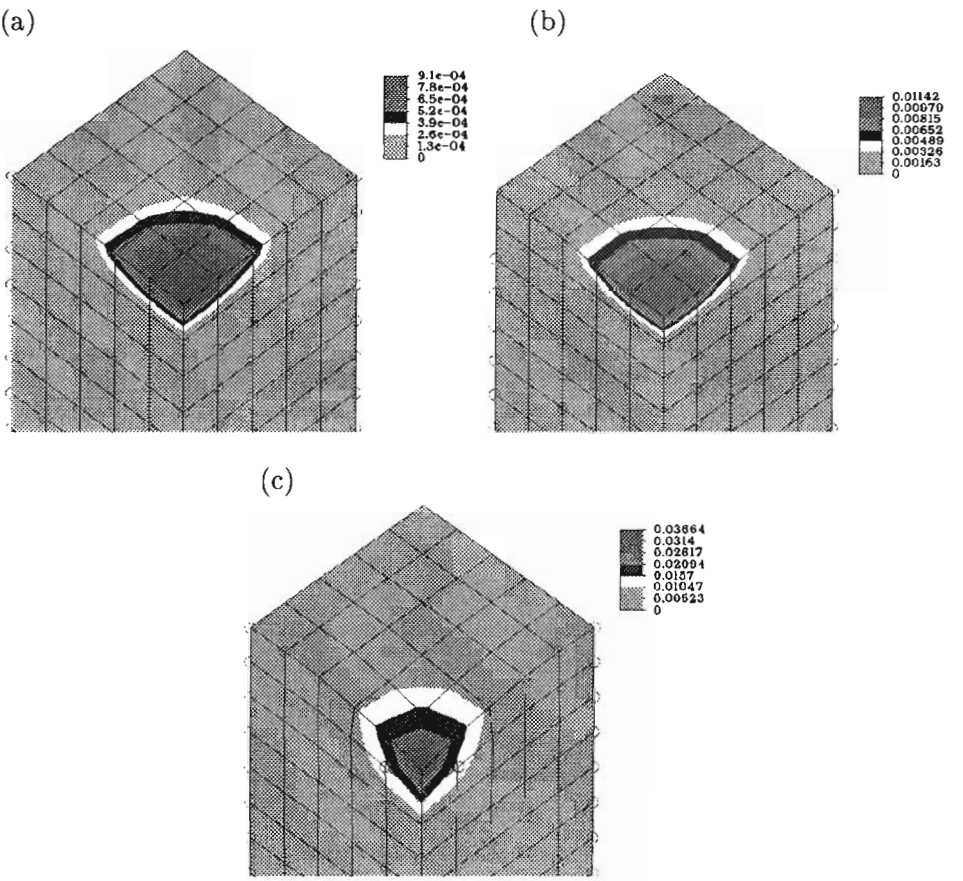

Fig. 2. Development of AWJ kerf with respect to time (abrasive particle is removed for clarity); (a) $t = 0.23\,\mu$s, (b) $t = 0.27\,\mu$s, (c) $t = 0.37\,\mu$s

The impact occurs after only $0.23\,\mu$s, Fig.2a, due to high AWJ speed of 400 m/s. At the cutting interface, there is a strong interaction between the

AWJ and the highly deformable layer of the workpiece. The abrasive particle interchanges its high momentum with the workpiece surface and as a result, deformation of the workpiece surface propagates. The severely deformed AWJ kerf continues its displacement downwards and goes into severe plastic deformation which is observed in Fig.2b. It is clearly seen from the figure that the workpiece deformation rises sharply in a very short time from (a) to (b). As the abrasive particle penetrates into the workpiece material, the AWJ kerf deepens and becomes narrower, Fig.2c. It is clear from the figure that the plastic deformation is very localized in the area of impact. This is considered to be one of the most important advantages of AWJM over the laser beam or plasma beam machining, which both induce a heat-affected zone around the cut area. However, the workpiece surface away from the jet impact region is not suffering from severe deformation.

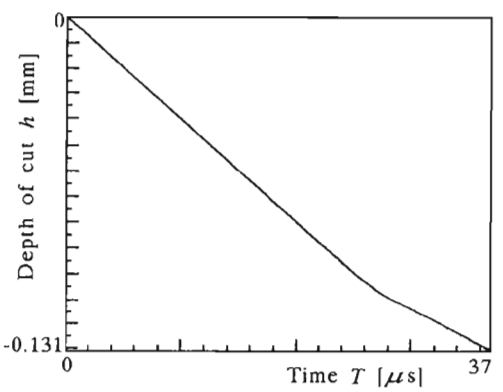

Fig. 3. Development of the depth of cut with time

The development of the depth of cut with time is shown in Fig.3. It is seen from the figure that, shortly after the initial impact period which is characterized by a large depth of the cut, the rate of deformation decreases. As a result, the depth of cut increases then at a slower rate. This observation occurs because AWJ loses its velocity as it penetrates into the workpiece material, causing a decrease in both the workpiece erosion rate and the surface quality towards the jet exit. Compared to the results of Hashish (1984a, 1988), the present results provide a better insight into the mechanism of interaction between the abrasive particle and the workpiece surface at the early stage of impact. Hashish based his analysis on macro-scale erosion, whose least time step used is 1 ms, whereas here it is based on micro-scale erosion in which the least time step is $0.01\,\mu$s.

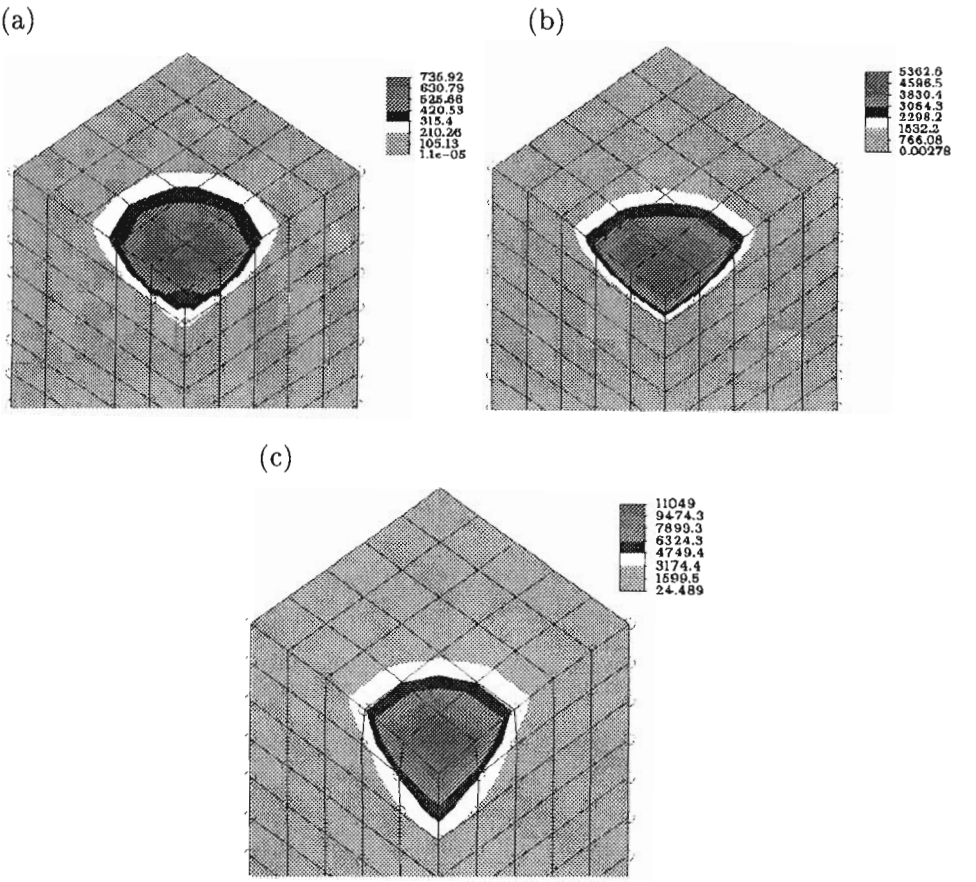

Fig. 4. Development of von Mises stresses as a result of AWJ impact; (a) $t = 0.23\,\mu$s, (b) $t = 0.27\,\mu$s, (c) $t = 0.37\,\mu$s

The impact of the abrasive particle on the workpiece surface causes peak loads which produce extremely high stresses causing local plastic deformation at the point of impact. Consequently, for a short time, intensive stresses that frequently produce a local site of damage develop in the workpiece material. In ductile materials, as in the present case, where the primary failure mechanism is plastic flow, the damage appears in the form of a conical crater around the impact site with the apex located exactly in the center. Figure 4 shows the results of the flow stresses acting at the cutting interface. The impact region is subject to high plastic compressive stresses, which exceed the rupture strength of the workpiece material causing local plastic deformation. It is seen that the maximum stress lies far away from the center of the impact site, Fig.4a. As the

abrasive particle penetrates into the workpiece material, the flow stress region decreases and the position of the maximum flow stress shifts inwards to the center of the impact site. The stress wave induced in the workpiece material as a result of the initial impact is clearly seen, Fig.4a. At a later stage, Fig.4b, stress waves propagate into the workpiece causing further plastic flow.

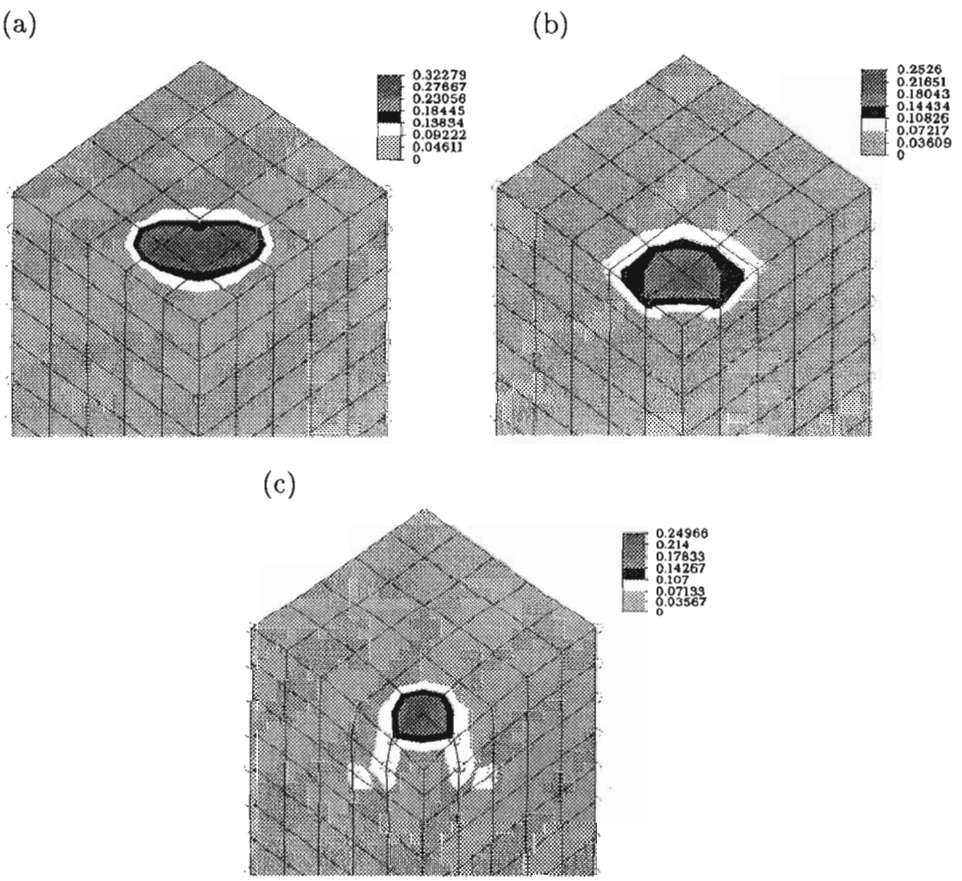

Fig. 5. Development of strains with time from the early impact; (a) $t = 0.23\,\mu$s (step 23), (b) $t = 0.27\,\mu$s, (c) $t = 0.37\,\mu$s

Figure 5 clearly shows that a comparatively wide region of compressive plastic strains develops along the AWJ kerf as soon as the abrasive particle impinges the workpiece surface, Fig.5a. This region moves to the center of the impact site, Fig.5b. As the abrasive particle penetrates into the workpiece material, Fig.5c, plastic strains concentrate along the kerf, especially in the center of the site of impact which suffers excessive platic deformation. It is

apparent that the plastic deformation is localized around the center of the impact site. This is consistent with the previous findings which stated that the strains occurring in erosion must be very large, and in addition, the surface will become work-hardened by the eroding particles (Finnie, 1995). It is clearly seen from the figure that a residual plastic strain appears in the area surrounding the AWJ kerf. These strains are large on the inner edge of the kerf, and they decrease rapidly as we move away from the kerf. This plastic strain distribution at various stages of abrasive particle impact, sheds some light on the development of the AWJ kerf and the accumulation of plasticity.

4. Conclusions

As a result of the present elastic-plastic dynamic FE model of the abrasive waterjet machining (AWJM) impact, the following conclusions could be drawn:

- There is a strong interaction between the AWJ and the highly deformable layer of the workpiece where the plastic deformation is localized. The workpiece deformation sharply rises in a very short time. Shortly after the initial impact period, the rate of deformation decreases.
- High compressive stresses are generated at AWJ cutting interface. These stresses reach values that exceed the compressive rupture strength of the material under high strain rate erosion loading causing the material to flow. This leads to severe local plastic deformation.
- As the abrasive particle penetrates into the workpiece material, the plastic strains increase sharply along the AWJ kerf, especially in the center of the site of impact which suffers excessive plastic deformation. This deformation is localized around the center of the impact site.

The paper is a result of the project No. 7 T08E 021 16 of the State Committeee of Scientific Research (KBN), Poland

References

1. BLICKWEDEL H., GUO N.S., HAFERKAMP H., LOUIS H., 1991, Prediction of Abrasive Jet Cutting Performance and Quality, *Proceedings of the 10th International Conference on Jet Cutting Technology*, BHR group, pp.163

2. CHEN L., SIORES E., WONG W.C.K., 1998, Optimizing Abrasive Waterjet Cutting of Ceramic Materials, *Journal of Materials Processing Technology*, **74**, 251-254

3. FINNIE I., 1995, Some Reflections on the Past and Future of Erosion, *Wear*, **1**, 186-187

4. GOLDSMITH W., 1999, Bouncing from One Collision to the Next, *Applied Mechanics Review*, **52**, 8, p.R27

5. HASHISH M., 1984a, A Modeling Study of Metal Cutting with Abrasive Waterjets, Transactions of the ASME, *Journal of Engineering Materials and Technology*, **106**, 1, p.88

6. HASHISH M., 1984b, Cutting with Abrasive Waterjets, *Mechanical Engineering*, **106**, p.60

7. HASHISH M., 1988, Visualization of the Abrasive-Waterjet Cutting Process, *Experimental Mechanics*, pp.159

8. HASHISH M., 1989, A Model for Abrasive-Waterjet (AWJ) Machining, *Transactions of the ASME, Journal of Engineering Materials and Technology*, **111**, p.154

9. HASSAN A.I., KOSMOL J., 1997, An Overview of Abrasive Waterjet Machining (AWJM), *Prace Naukowe Katedry Budowy Maszyn*, Politechnika Śląska, Gliwice, 2/97, 181-205

10. HASSAN A.I., KOSMOL J., 1998, A Preliminary Finite Element Model of Waterjet Machining (WJM), *Proceedings of the Conference: III Forum prac badawczych "Kształtowanie części maszyn przez usuwanie materiału"*, Koszalin, Poland, 1-3, p.235

11. HOOGSTRATE A.M. ET AL., 1997, Opportunities in Abrasive Water-Jet Machining, *Annals of the CIRP*, **46**, 2, p.697

12. PAUL S., HOOGSTRATE A.M., VAN LUTTERVELT C.A., KALS H.J.J., 1998, Analytical Modeling of the Total Depth of Cut in the Abrasive Waterjet Machining of Polycrystalline Brittle Materials, *Journal of Materials Processing Technology*, **73**, p.206

13. SIORES E., WONG W.C.K., CHEN L., WAGER J.G., 1996, Enhancing Abrasive Waterjet Cutting of Ceramics by Head Oscillation Technique, *Annals of the CIRP*, **45**, 1, p.327

14. ZENG J., KIM T.J., 1996, An Erosion Model of Polycrystalline Ceramics in Abrasive Waterjet Cutting, *Wear*, **193**, 2, p.207

Modelowanie obróbki strumieniem wodnościernym metodą elementów skończonych

Streszczenie

W artykule przedstawiono pierwsze podejście do modelowania obróbki strumieniem wodnościernym metodą elementów skończonych. Celem badań jest próba wyjaśnienia zjawisk występujących na styku ścierniwa i przedmiotu obrabianego. Ten nowy model w sposób precyzyjniejszy uwzględnia właściwości materiału poddanego dynamicznym obciążeniom, co we wcześniejszych modelach nie było uwzględniane. W modelu tym nie trzeba definiować początkowej siły działającej na ścierniwo (jak to miało miejsce w poprzednich modelach), ponieważ jest ona automatycznie obliczana w każdym kroku czasowym. Wyniki symulacji pokazują, że MES jest bardzo dobrym narzędziem do przewidywania reakcji pomiędzy ścierniwem i przedmiotem obrabianym oraz głębokości skrawania.

Manuscript received March 28, 2000; accepted for print June 6, 2000